Interaction of electromagnetic fields with the environment/Interaction du champ électromagnétique avec l'environnement

Modelling of electromagnetic wave interactions with the human body

Man-Faï Wong [*], Joe Wiart

France Télécom Research & Development, 92794 Issy-les-Moulineaux, France

Available online 1 September 2005

Abstract

Electromagnetic modelling plays a more and more important role in the study of complex systems involving Maxwell phenomena, such as the interactions of radiowaves with the human body. Simulation then becomes a credible means in decision making, related to the engineering of complex electromagnetic systems. To increase confidence in the models with respect to reality, validation and uncertainty estimation methods are needed. The different dimensions of model validation are illustrated through dosimetry, i.e., quantification of human exposure to electromagnetic waves. ***To cite this article: M.-F. Wong, J. Wiart, C. R. Physique 6 (2005).***
© 2005 Académie des sciences. Published by Elsevier SAS. All rights reserved.

Résumé

Modélisation des interactions des ondes électromagnétiques avec les personnes. Les modèles électromagnétiques issus des équations de Maxwell gagnent en maturité et font de la simulation une alternative crédible dans les prises de décision liées aux systèmes électromagnétiques complexes. Pour renforcer la confiance en les modèles vis-à-vis de la réalité, des méthodes de validation et d'estimation des incertitudes sont nécessaires. Différentes dimensions de la problématique de la validation des modèles sont abordées à travers la dosimétrie, ou quantification de l'exposition des personnes au champ électromagnétique. ***Pour citer cet article : M.-F. Wong, J. Wiart, C. R. Physique 6 (2005).***
© 2005 Académie des sciences. Published by Elsevier SAS. All rights reserved.

Keywords: Electromagnetic wave interactions; Dosimetry; Validation; Uncertainty

Mots-clés : Interactions ondes électromagnétiques ; Dosimétrie ; Validation ; Incertitudes

1. Introduction

Nowadays, electromagnetic (EM) models derived from different approximations of Maxwell equations are more and more used in electromagnetic systems engineering: microwave circuits and antennas embedded in their environment, electromagnetic compatibility, propagation in random media, dosimetry. The use of simulation in place of or in complement to measurement, leads to qualify the EM models in terms of validity and confidence. Validation activities aim at evaluating their accuracies and their reliabilities. Prediction quality plays a crucial role in decision making related to performance, reliability, and safety of systems. The field of the interactions of EM waves with the human body is remarkable in this respect. With the tremendous

---

development of ubiquitous wireless communications, especially mobile phones, questions have arisen about the potential effects of radiowaves on health. Simulation tools have been used to assess the compliance of the radio systems with respect to defined limits for the safety of people [1]. They have also been used to derive standards for the measurement assessments [2,3]. Typically, absorption of the EM waves in tissue has to be evaluated. Measurement is invasive while simulation can give 3D cartography of absorbed power. However, absolute results are required and it can be very challenging when the environment is not perfectly known. Confidence in the models is a key issue, in particular, when health issues are concerned.

2. Which models?

Different EM models can be derived. First, according to the system's size in terms of wavelength, different approximations of Maxwell equations can be used: quasi-static when the size is small compared to wavelength, asymptotic high frequencies when the size is large compared to wavelength. When the size is comparable to the wavelength as it is the case for a mobile phone close to a head, full-wave techniques are used. The classical techniques, Finite Element Method (FEM), Method of Moments (MoM), Transmission Line Matrix (TLM) are applicable. However, the Finite Difference Time Domain (FDTD) [4,5] is the technique of choice, as it is able to tackle a large grid comprising realistic and highly heterogeneous models of human tissue coming from MRI (Magnetic Resonance Imaging). Each model has its range of validity, using it out of its scope is a typical error in the (mis)use of a model.

However, the higher the fidelity to the reality, the higher the computational cost (Fig. 1). This means that simpler models can be useful for dedicated purposes. For example, instead of modelling a realistic head and mobile phone, it could be interesting to simplify this as a sphere with a half-wavelength dipole. Firstly, simpler cases can give more insight in the phenomena, parametric studies may be easier, thus giving high qualitative and pedagogical values to them. Secondly, they can provide very accurate analytical results for validation of numerical EM models as shown below. Another example is provided at the other end of the radio link of a mobile network, i.e., base station antennas. In this case for compliance purposes, the incident isotropic

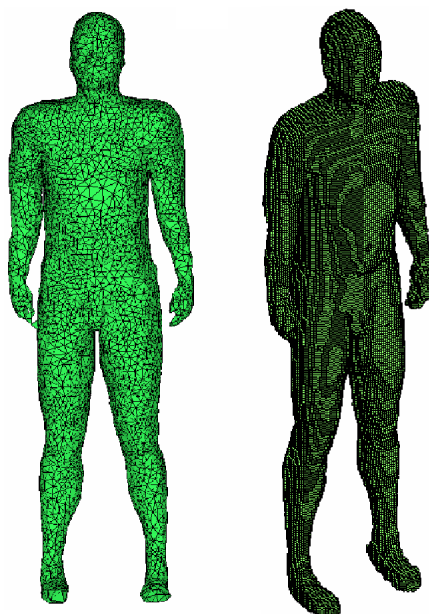Fig. 1. Fidelity/reality versus computation cost.

Fig. 2. Examples of human bodies meshes: unstructured/FEM (left), structured/FDTD (right).

field has to be evaluated for comparisons to limits. A model based on far field gain can be a fast and overestimating model compared to a more accurate near field model. Models giving bounds are useful for quick prototyping and first analyses.

Returning to full-wave EM models, after that a model has been properly verified, the major issue is convergence of the solutions with respect to mesh refinement or series truncation. This leads to a convergence error of the numerical method. In bioelectromagnetics, FDTD is perfectly suited for tissue modelling with its orthogonal grid. However, the drawback is a stair-casing error of curved geometries. Brute force refinement is not practical. Thus, subgridding techniques have been investigated [6–11] and lately, new conforming FDTD [12], FEM or Finite Volume [13] are studied in order to improve the accuracy with respect to geometry details. Fig. 2 shows examples of unstructured and structured meshes for human bodies.

Validation is essential to qualify a model. It can be done by comparison with canonically known analytical solutions, intercomparisons between codes or methods and more desirable comparisons with measurement. A benchmark has been carried out between France Telecom (FT) and Deutsche Telekom (DT) in the framework of a Eurescom project. FT uses its own non-uniform FDTD code and DT uses the commercially available code MAFIA[TM] based on Finite Integration Technique (FIT) [14] which is very close to FDTD. To compare the results given by the different programs, a limited number of canonical problems, designed to have dimensions similar to those of the human head have been used by the two groups and the specific absorption rate (SAR), electric (E) and magnetic (H) fields results compared. Commonly used in bioelectromagnetics, the SAR measures the power absorbed by tissues, its unit is W/kg and can be calculated from the *E* field as:

$$SAR = \frac{\sigma |E|^2}{\rho}$$

where σ (S/m) is the conductivity and ρ (kg/m^3) is the density of the tissue. The case of a homogeneous sphere illuminated by a plane-wave of 10 W/m^2 (Fig. 3), whose electromagnetic solution is given by Mie, has been selected since it allows not only an inter-comparison between tools, but also a comparison to an exact solution. The sphere representing the head has a radius *r* of 0.1125 m (i.e., diameter = 0.225 m) and the centre of the sphere has been located at the centre of a cell. The dielectric properties of the sphere are those of the brain given by the FCC web site [15]: relative permittivity is $\varepsilon_r = 45.7691$, and conductivity is $\sigma = 0.769$ S/m at 909 MHz (nominal 900 MHz), and respectively $\varepsilon_r = 43.6068$, $\sigma = 1.1355$ S/m at 1764.7 MHz (nominal 1800 MHz). The field and SAR values are compared at 6 locations. Different types of grids are used: different grid step sizes and uniform and graded meshes (Fig. 3). A sample of the results is shown in Fig. 4. For DT results, the mesh is 1 mm in the area of interest and larger in areas not of interest. There is no graded transition. FT#1 results use DT mesh. FT#2 results are for a non-uniform mesh with smaller mesh size of 1 mm. FT#3 results use a uniform 1 mm mesh. These results are compared to the Mie solution. At the point 3 (Fig. 3), which is the closest to the surface, the difference is around 10% for 5 mm non-uniform mesh, while it is less than 4% for 1 mm non-uniform mesh.
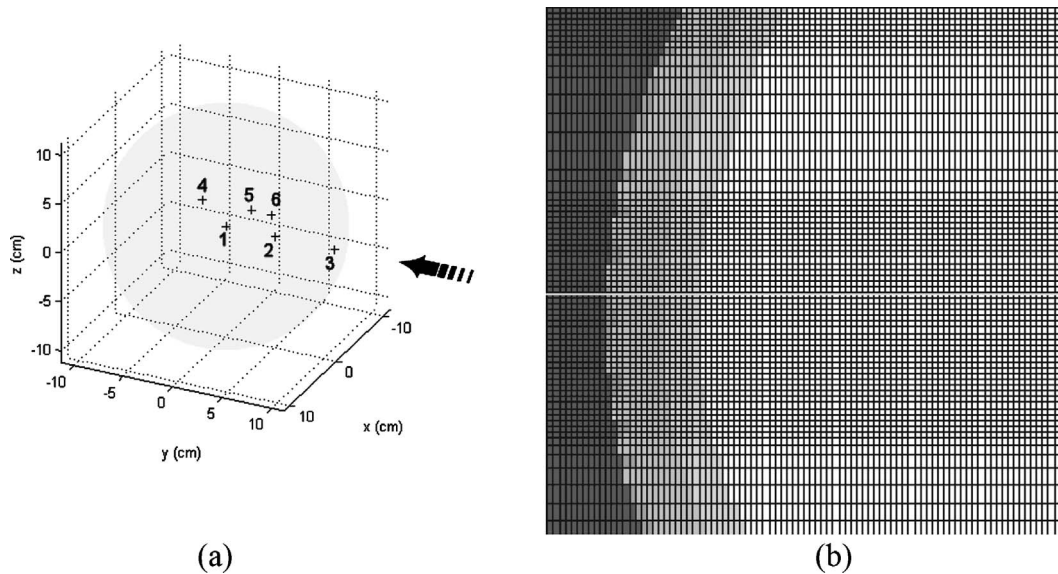
(a)   (b)

Fig. 3. Sphere illuminated by plane wave along y-axis: (a) reference points $1 = (0, 0, 0)$, $2 = (0, 5, 0)$, $3 = (0, 11, 0)$, $4 = (5, 0, 5)$, $5 = (5, 5, 5)$, $6 = (5, 7, 5)$; (b) non-uniform mesh of the sphere.
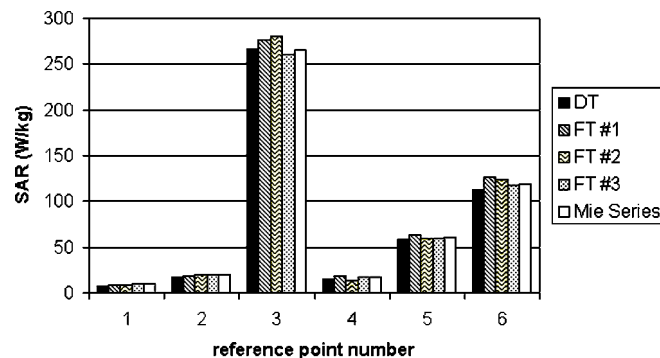

Fig. 4. Comparisons of SAR versus Lab and location at 1764.7 MHz.

At this point, it is worth mentioning that although measurement is considered as a reference, it has its own errors and biases. In electromagnetics, the EM fields can be measured with probes or antennas but they are of finite size which tend to average the results. When measuring SAR within phantom for compliance testing, the probes are not calibrated to measure very close to the interfaces between the equivalent liquid and the phantom shell [16]. For environmental in situ measurement of the exposure induced by base station antennas, multipath propagation conditions make the field highly variable in time and space [16]. In order to have reproducible measurements, special spatial averaging methods are needed [17].

3. Confrontation with reality

When an EM model has been validated, the discrepancies between prediction and reality are coming from the input data, i.e., the sources, the geometry and material properties of the objects. The main limitation is then the estimation of the input parameters. The output of the model is observables that are meant to replace actual measurements. Fig. 5 shows a diagram of a model with its inputs and output and the sources of uncertainties.

Regarding observables, they are global or local. Local observables are direct EM fields, solutions of Maxwell equations, or derived locally as local SAR which is defined as the integration of point SAR over 1 g or 10 g of tissues. These observables are more sensitive, dependent of the mesh refinement and difficult to compare. Global observables, such as total absorbed power,
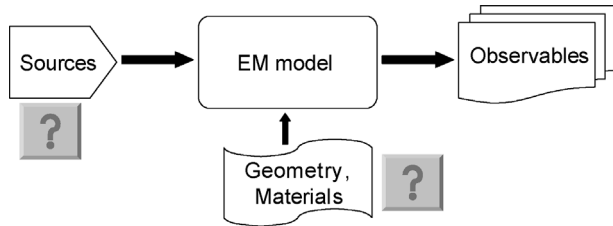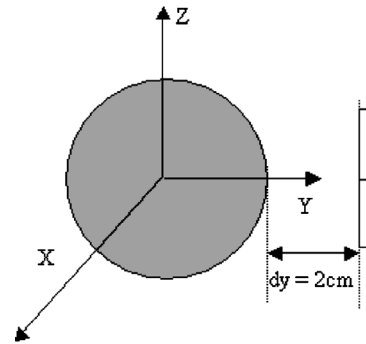
Fig. 5. Model as a transfer function.
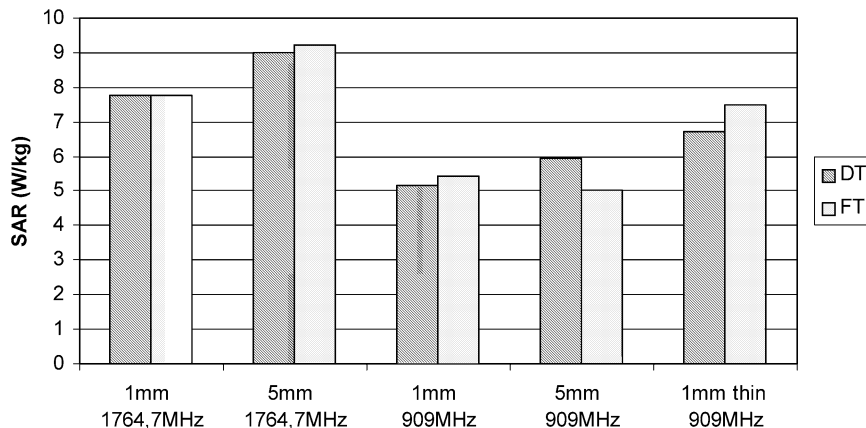

Fig. 6. A sphere illuminated by a dipole.

Fig. 7. Comparisons of local SAR versus frequency, mesh size and thick/thin source.

power budget, whole body SAR (i.e., the total absorbed power in the body divided by weight) present a better agreement with reality as they can sometimes be shown as variational quantity with respect to the fields.

Quality of an EM model can be also assessed through its ability to give first qualitative results which is the minimum requirement, then incremental or distribution kind of results, and finally absolute value results. For example, consider the radiation pattern of an antenna, if you consider a 3D view of it, the information is essentially qualitative. Then one can plot a normalized radiation pattern with respect to angle. The distribution is often achieved. Finally the agreement has to considered with the absolute gain. The definition of metrics is very important for the comparison [18,19]. In the comparison of the absolute value of absorbed power by tissues from a source, the normalization of the field values may be either done by the source current or voltage or by the emitted power.

Source modelling is indeed crucial when absolute values are needed as the source itself has to be as close as possible to the reality. However, the excitation can be arbitrary provided that post-processing can be used to correct the results. Typically, this approach is carried out when EM system parameters, like S-parameters, are needed. So called de-embedding techniques used for measurement are applied in simulations [20,21]. Within the benchmark between FT and DT, the case of a dipole close to a sphere has also been tested (Fig. 6). FT uses a voltage source within the gap of the dipole. DT uses a current source. Time variations are also different: a pulse for FT and a sinus for DT. As usual with FDTD, harmonic results are obtained by Fourier transform. The results are normalized relative to the emitted power, which corresponds to reality. Although the EM field is linearly dependent on the current or voltage, the normalization to the current or voltage is not supported in the real condition. Furthermore, results are more difficult to compare because the impedance or admittance which are related to the power are very sensitive to the source modelling. Fig. 7 shows the comparisons between FT and DT results for local SAR at point 3. The 1 mm mesh size is non-uniform while the 5 mm is uniform. The wire of the dipole is either a thick model, 1-cell thick metal, or a simple thin-wire model where the tangential component along the wire is forced to zero. The most important difference is 15% for the 5 mm mesh at 909 MHz. The lack of information about the internal components of installed base station antennas makes the evaluation of human exposure in their vicinity uncertain from the source. In order to get very accurate antenna models based on measurement, inverse problem solutions can be built from the knowledge of the 3D radiation pattern [22].
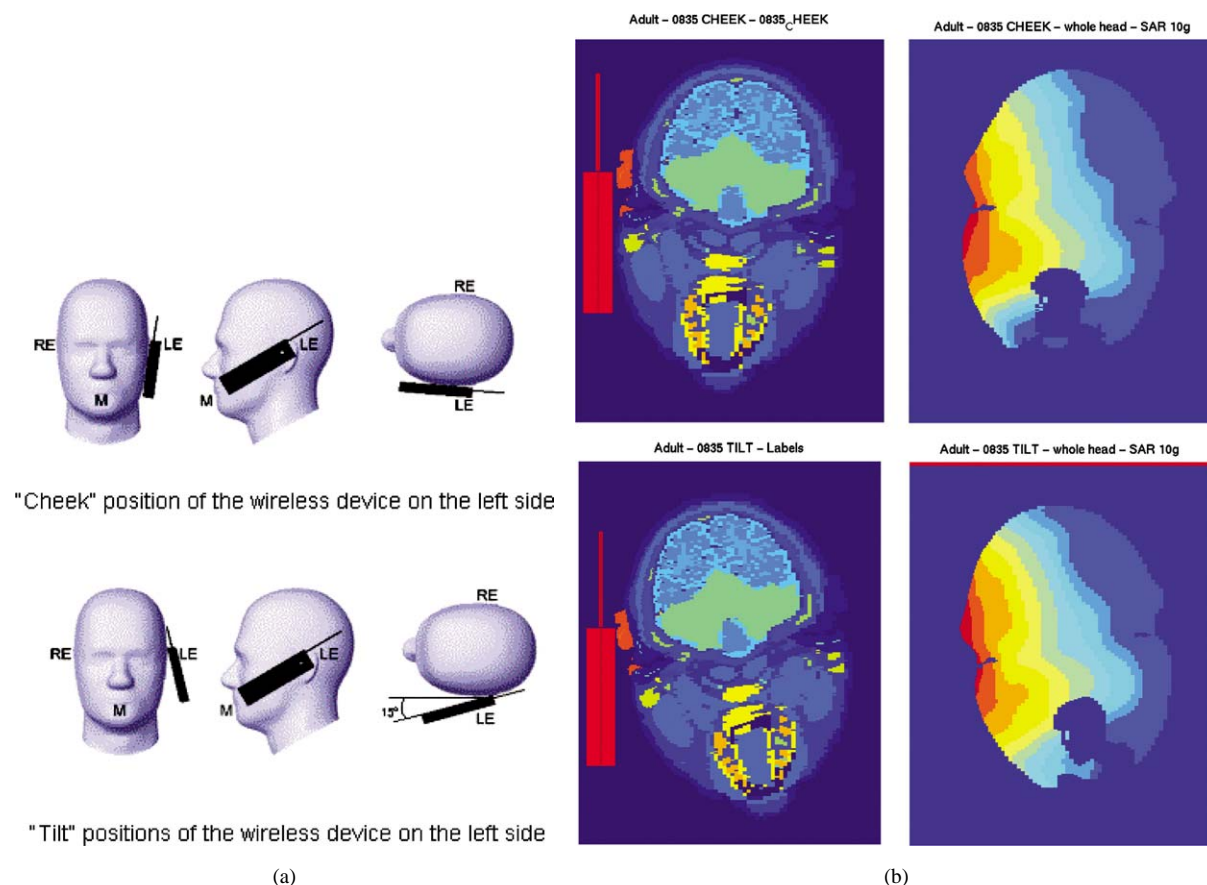
Fig. 8. (a) Phone positioning, cheek and tilt positions; (b) SAR distributions for cheek and tilt positions.

Dielectric properties of the objects in a simulation may be not very well known too. Radiopropagation or human exposure in the urban environment comprising buildings, rooftops, chimneys are typical examples. A remedy is to optimize the dielectric parameters such that the prediction is close to measurement [23]. Therefore, a kind of calibration of the model is done. In the interactions of radiowaves with human bodies, dielectric properties of the tissues vary versus individual and age.

Finally, the geometry can lead to uncertainties. The retrieval of geometry from CAD files for meshing and simulation is a known issue. The relative positioning of a mobile phone and a head is being carried out in an international level coordinated by IEEE SCC 34: SAR estimation using computational methods. Different labs are calculating the defined positions and results will be compared (Fig. 8(a)). The interactions of EM waves with human bodies depend on morphology. Mobile phones are widely used by all, including children. Important questions are raised about the nature and degree of absorption by children as a function of their age and their morphology. A research program has been set up to investigate these questions [24–26]. Moreover, the position of a human body can modify the distribution and absorption of EM waves: raising the arms when standing or sitting is like modifying the height of an antenna.

4. Uncertainty management

The uncertainties or variabilities of the input parameters lead to uncertainties or variabilities of the results. However, the uncertainty can be propagated through the model. Indeed, it is the strength of simulation that one can play 'what if' scenarios, give sensitivity analysis, reliability or yield analysis. Then such analyses can be related to risk assessment for decision making. This means quantifying not only the value of some prediction, but also the error bounds and confidence levels associated with such predictions. A first illustration is the case of mobile phone positioning in the IEEE work discussed previously. Fig. 8(b) shows the SAR distribution for tilt and cheek positions. The outcome will be the variation of SAR between the positions but also the repeatability of the results across different labs.

In the definition of a standardized method for compliance testing [2,27], simulation has been advantageously used to support the harmonised measurement protocol. In order to test mobile phones, SAR is evaluated within a phantom which should be representative of a human head. The shape being defined, the dielectric properties of the filling liquid in which a probe is displaced to measure the distribution of SAR has to be defined. The equivalent liquid, which is homogeneous, has to provide about the same value for the peak SAR than in a real heterogeneous head. The SAR is evaluated by varying the conductivity and permittivity of a homogeneous liquid and compared to the results of a heterogeneous head with or without ears. Fig. 9 shows two slices of the 2-D surface of SAR versus the 2 parameters at 1800 MHz. Values indicated on the figures are the variations of SAR for 10% variation of conductivity or permittivity. The SAR is more sensitive to conductivity than to permittivity: conductivity variations are about 2 times those for permittivity. Variations of SAR over 1 g are about 2 times those over 10 g. It is also shown that matching the SAR in homogeneous liquid with a heterogeneous model with an ear is difficult within these variation ranges of the parameters.

Instead of defining a new equivalent liquid for testing mobile phones when they are body worn, comparisons are made between the homogeneous medium and layered media representing the torso of a human body, in different parts of a body. The different multilayer structures have been extracted from Visible Human [28]. In case of an incident plane wave, the SAR is assessed using a simple analytical multilayer model to build the histogram of the SAR values with the different multilayers (Fig. 10). The arrow in the right hand figure corresponds to the homogeneous result. A factor 2 is found to be sufficient enough to overestimate all the heterogeneous results. In this case, with the simple and fast model, a Monte Carlo approach can be also used to study the SAR variability versus the variability of multilayers thicknesses.
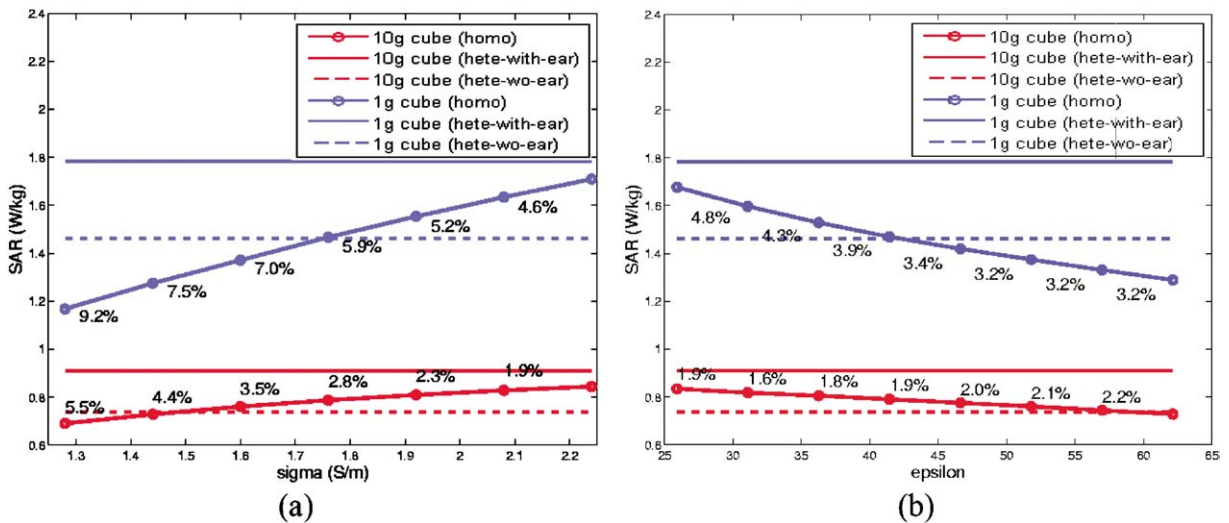

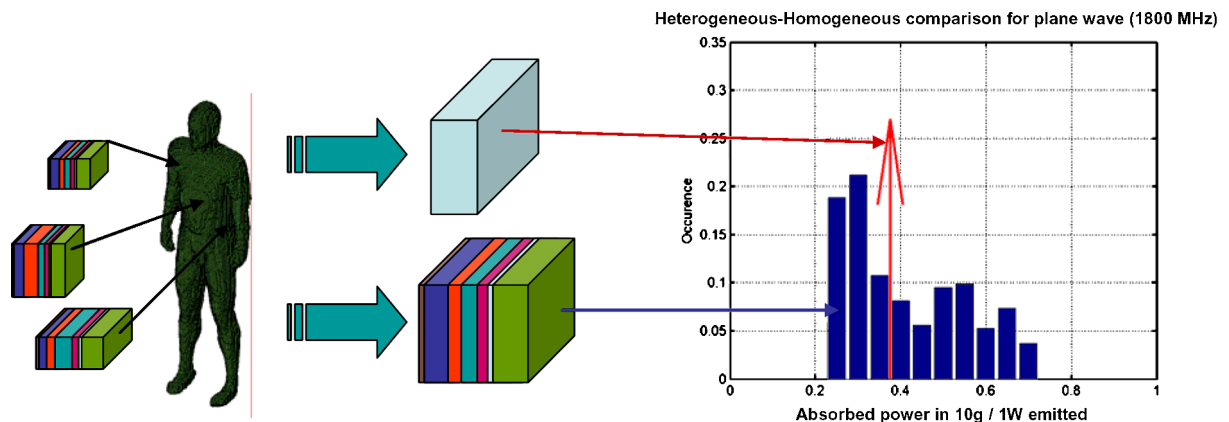Fig. 9. (a) SAR versus conductivity; (b) SAR versus permittivity.

Fig. 10. SAR statistic distribution for different multilayer structures.

Table 1
Scaled human body models of different shapes

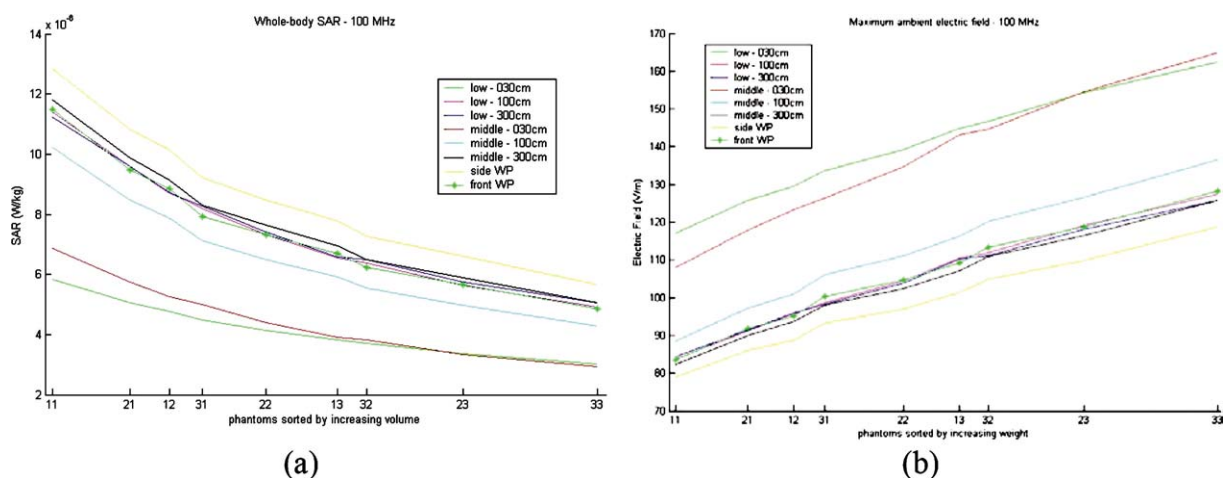| Model numbering	Height (m)	Weight (kg)
11	1.598	48.85
12	1.598	63.84
13	1.598	84.84
21	1.741	58.98
22	1.741	75.77
23	1.741	100.70
31	1.882	67.76
32	1.882	88.55
33	1.882	117.67

Fig. 11. (a) SAR versus human body volume; (b) maximum ambient field versus human body volume.

A last example is given here with the influence of human body shape on the whole body SAR which is a part of the FT-DT project. From statistical data about the height and Body Mass Index (BMI) of individuals, a whole body model is deformed. BMI is a measure of body proportion, used medically as a clinical indicator of underweight, correct weight, overweight, or obesity, defined as

$$BMI = m/h^2$$

for body mass m and body height h. A BMI under 18 is considered an indicator of being underweight; a BMI between 18.0 and 25.0 is the normal range; a BMI of 25.0 to 29.9 is considered an indicator of overweight and a BMI greater than 30 indicates obesity. The mean height is 174.1 cm and the standard deviation is 7.1 cm. The retained value for minimum, mean and maximum BMI are 19.13 kg/m^2, 25 kg/m^2 and 33.22 kg/m^2. This range of variations enables the building of 9 scaled models of Zubal human body [29]. Two times the standard deviation is taken for the height. See Table 1. Different incident waves are illuminating the different size models at 100 MHz: plane waves from the front or the side and an array of 2 dipoles. Fig. 11(a) shows the results for the whole body SAR with respect to the volume of the different bodies. The variation is quite smooth, as expected the higher is the volume, the higher is the weight and the lower is the SAR. Knowing the SAR for a given incident field level, the inverse useful relation, giving the level of ambient incident field above which the absorption exceeds the limits of safety recommendations (Fig. 11(b)).

5. Conclusion

Computational electrodynamics is a rapidly evolving field which is more and more used in engineering analysis and design. However, uncertainty estimates are required, specially when interactions with the environment are involved. This is the case in the analysis of EM wave interactions with the human body, where a purely deterministic approach integrates more and more probabilistic and stochastic elements. Uncertainties induced by the lack of knowledge of the environment have to be estimated

in order to manage them and eventually to evaluate and manage risk. In the same time, deterministic models have to deal with convergence of the numerical methods with larger and larger models. Estimation of convergence error and mesh adaptivity needs to be developed. As well, techniques to estimate uncertainties, to calculate model from uncertainty, are to be developed. The coupling in simulation tool of measurement derived model and computational model will help the predictions to agree with the real life world. The propagation of uncertainties need more sophisticated methods than pure and brute-force Monte Carlo simulations, which are not practicable, even though computing power also progresses rapidly.

Acknowledgements

References

[1] ICNIRP Guidelines, Guidelines for limiting exposure to time-varying electric, magnetic, and electromagnetic fields (up to 300 GHz), Health Phys. 74 (4) (1998).
[2] CENELEC EN50361, Basic standard for the measurement of Specific Absorption Rate related to human exposure to electromagnetic fields from mobile phones (300 MHz – 3 GHz), 2001.
[3] CENELEC EN50383, Basic standard for the calculation and measurement of electromagnetic field strength and SAR related to human exposure from radio base stations and fixed terminal stations for wireless telecommunication systems (110 MHz to 40 GHz), 2002.
[4] A. Taflove, Computational Electrodynamics. The Finite Difference Time Domain Method, Artech House, Boston, 1995.
[5] J. Wiart, S. Chaillou, Z. Altman, S. Drago, Calculation of the power deposited in tissues close to a handset antenna using a non-uniform FDTD, in: F. Bersani (Ed.), Electricity and Magnetism in Biology and Medicine, Second World Congress Following BEMS, Kluwer, New York, 1999.
[6] M. Okoniewski, E. Okoniewska, M.A. Stuchly, Three-dimensional subgridding algorithm for FDTD, IEEE Trans. Antennas Propagat. 45 (3) (1997) 422–429.
[7] P. Thoma, T. Weiland, A consistent sungridding scheme for the finite difference time domain method, Internat. J. Numer. Model. 9 (1996) 359–374.
[8] S. Chaillou, J. Wiart, W. Tabbara, A subgridding scheme based on mesh nesting for the FDTD method, Microwave Opt. Technol. Lett. 22 (3) (1999) 211–214.
[9] M. Bonilla, M. Wong, V. Fouad Hanna, A finite element formulation for FDTD subgridding, Microwave Opt. Technol. Lett. 32 (2) (2002) 104–108.
[10] G. Carat, R. Gillard, J. Citerne, J. Wiart, An efficient analysis of planar microwave circuits using a DWT-based Haar MRTD scheme, IEEE Trans. Microwave Theory and Techniques 48 (12) (2000) 2261–2270.
[11] M. Marrone, R. Mittra, A theoretical study of the stability criteria for hybridized FDTD algorithms for multiscale analysis, IEEE Trans. Antennas Propagat. 52 (8) (2004) 2158–2167.
[12] N. Chavannes, N. Kuster, A novel 3D CPFDTD scheme for modeling grid nonconformally aligned transmitter structures, IEEE Trans. Antennas Propagat. 52 (5) (2004) 1324–1334.
[13] Headexp, Realistic numerical modelling of human head tissues exposure to electromagnetic waves from mobile phones, http://www-sop.inria.fr/caiman/personnel/Stephane.Lanteri/headexp/headexp.html, 2003.
[14] T. Weiland, Time domain electromagnetic field computation with finite difference methods, Internat. J. Numer. Model. 9 (1996) 295–319.
[15] FCC website, tissues dielectric properties http://www.fcc.gov/fcc-bin/dielec.sh, 1997.
[16] J. Wiart, Métrologie des interactions des ondes radioélectriques avec les tissus vivants, Bulletin du Bureau National de Métrologie 2004-3 (126) (2004) 48–55.
[17] E. Larchevêque, C. Dale, M.F. Wong, J. Wiart, Analysis of electric field averaging for in situ radiofrequency exposure assessment, IEEE Trans. Vehicular Technol., in press.
[18] A. Williams, A. Duffy, M. Woolfson, T. Benson, A powerful new technique for the quantitative validation of modeled and experimental data, Microwave Optical Technol. Lett. 17 (5) (1998) 284–287.
[19] J. Rautio, The microwave point of view on software validation, IEEE Antennas Propagat. Magazine 38 (2) (1996) 68–71.
[20] B. Linot, M.F. Wong, V. Fouad Hanna, O. Picon, A numerical TRL de-embedding technique for the extraction of S-parameters in a 2.5D planar electromagnetic simulator, in: IEEE MTT-S Internat. Microwave Symposium, vol. 2, Orlando, USA, May 1995, pp. 809–812.
[21] Z. Lei, W. Ke, Short-open calibration technique for field theory-based parameter extraction of lumped elements of planar integrated circuits, IEEE Trans. Microwave Theory and Techniques 50 (8) (2002) 1861–1869.
[22] A. Gati, Y. Adane, M. Wong, J. Wiart, V. Fouad Hanna, Inverse characterization of sources for the study of the environment interaction with electromagnetic fields, C. R. Physique (2005), in this issue.
[23] R. Matschek, A geometrical optics and uniform theory of diffraction based ray tracing optimisation by a genetic algorithm, C. R. Physique (2005), in this issue.

[24] J. Wang, O. Fujiwara, An examination of the theory and practices of planar near-field measurement, IEEE Trans. Antennas Propagat. 36 (6) (1988) 746–753.

[25] Adonis RNRT project website, http://www.tsi.enst.fr/adonis/.

[26] A. Hadjem, D. Lautru, C. Dale, M.F. Wong, V. Fouad Hanna, J. Wiart, Study of specific absorption rate (SAR) induced in two child head models and in adult heads using mobile phones, IEEE Trans. Microwave Theory and Techniques 53 (1) (2005) 4–11.

[27] Comobio RNRT project website, http://www.tsi.enst.fr/comobio/.

[28] The Visible Human Project website, http://www.nlm.nih.gov/research/visible/visible_human.html.

[29] I. Zubal, C. Harrell, E. Smith, Z. Rattner, G. Gindi, P. Hoffer, Computerized 3D segmented human anatomy, Med. Phys. 21 (2) (1994) 299–302.